ACS APPLIED MATERIALS & INTERFACES

Research Article

www.acsami.org

Instantaneous Pulsed-Light Cross-Linking of a Polymer Gate Dielectric for Flexible Organic Thin-Film Transistors

Soo Jin Kim,[†,∥] Mi Jang,[‡] Hee Yeon Yang,[∥] Jinhan Cho,[†] Ho Sun Lim,[§] Hoichang Yang,*[,‡] and Jung Ah Lim*[,∥]

[†]Department of Chemical and Biological Engineering, Korea University, 02841 Seoul, Korea

[‡]Department of Applied Organic Materials Engineering, Division of Nano-systems Engineering, Inha University, 22212 Incheon, Korea

[§]Department of Chemical and Biological Engineering, Sookmyung Women's University, 04310 Seoul, Korea

[∥]Center for Optoelectronic Materials and Devices, Korea Institute of Science and Technology, 02792 Seoul, Korea

Supporting Information

ABSTRACT: We report the instantaneous pulsed-light cross-linking of polymer gate dielectrics on a flexible substrate by using intensely pulsed white light (IPWL) irradiation. Irradiation with IPWL for only 1.8 s of a poly(4-vinylphenol) (PVP) thin film with the cross-linking agent poly(melamine-*co*-formaldehyde) (PMF) deposited on a plastic substrate was found to yield fully cross-linked PVP films. It was confirmed that the IPWL-cross-linked PVP films have smooth pinhole-free surfaces and exhibit a low leakage current density, organic solvent resistance, and good compatibility with organic semiconductor, and that they can be used as replacements for typical PVP dielectrics that are cross-linked with time and energy intensive thermal heating processes. The synchronization of the IPWL irradiation with substrate transfer was found to enable the preparation of cross-linked PVP films on large area substrates with a highly uniform capacitance. Flexible OTFT based on IPWL-cross-linked PVP dielectrics were found to exhibit good electrical performance that is comparable to that of devices with thermally cross-linked PVP dielectric, as well as excellent deformation stability even at a bending radius of 3 mm.

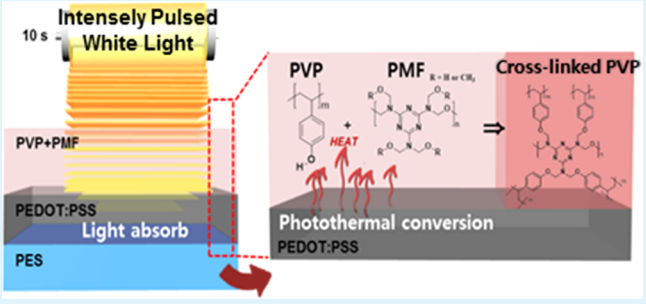

KEYWORDS: *intensely pulsed white light, cross-linking, gate dielectric, organic thin-film transistors, flexible substrate*

1. INTRODUCTION

The recent interest in flexible electronics has focused attention on organic or polymer based electronic materials such as organic semiconductors, conducting polymers, and polymer dielectric. These materials possess electronic functions and compatibility with flexible plastic substrates, as well as large area processability, and they are light in weight, which enables the realization of flexible electronic devices via low-cost, low-temperature fabrication processes. Of the various organic-based electronic devices, organic thin-film transistors (OTFTs) are fundamental components of a large number of electronic applications as diverse as radiofrequency identification (RFID), backplane circuitry of displays, sensors, and smart cards.[1−4] In the past decade, it has been pointed out that the low carrier mobility of OTFTs limits their practical utilization in these applications. However, in the laboratory research the recent combinatorial development of organic semiconductors with high carrier mobilities and suitable gate dielectrics with smooth surfaces and low leakage current densities has led to flexible OTFTs with improved carrier mobilities above 16 $cm^2V^{-1}s^{-1}$.[5−7] Nevertheless, from the viewpoint of the practical fabrication of flexible OTFTs, the development of low-temperature and large-area processes compatible with high throughput roll-to-roll production systems is still required. Of the various stages in the preparation of flexible OTFTs, the thermal treatment (i.e., thermal heating) commonly used for the structural development of organic semiconductors, sintering of metal nanoparticle-based electrodes, and the cross-linking of polymer gate dielectrics is inefficient, energy consuming, and the rate-determining step, so an alternative is needed that enables the use of low-temperatures and can be applied over a large area and at high processing speeds. Recently, much research effort has been devoted to the development of methods for the low-temperature sintering of conductive nanoparticles and the direct self-assembly of organic semiconductors without thermal treatment. However, the highly efficient cross-linking of polymer gate dielectrics has rarely been demonstrated.

The polymer gate dielectrics used in OTFTs are typically cross-linked systems in order to improve their chemical

Received: November 22, 2016
Accepted: March 15, 2017
Published: March 27, 2017

DOI: 10.1021/acsami.6b14957
ACS Appl. Mater. Interfaces 2017, 9, 11721−11731

resistance and reduce their leakage current. Of the polymer gate dielectrics reported to date, one of the most useful is cross-linked poly(4-vinylphenol) (PVP). In addition to the general advantages of polymer dielectrics such as solution processability and good mechanical flexibility, cross-linked PVP has good dielectric properties including a low leakage current, chemical resistance, and compatibility with various organic semiconductor.[8−11] In recent reports, cross-linked PVP has been also utilized as a matrix material for nanocomposites with high-k nanomaterials.[12−14] A cross-linked PVP dielectric layer is typically spun-cast from a solution of PVP and poly(melamine-*co*-formaldehyde) (PMF), which is a cross-linking agent, and then cross-linked at a high temperature of above 180 °C. However, this cross-linking temperature is unsuitable for flexible plastic substrates, which have low glass transition temperatures T_g < 150 °C. To overcome this drawback, various cross-linking systems comprised of PVP and cross-linkers have been demonstrated. Bao and co-workers reported the low-temperature cross-linking of PVP at 110 °C by using 4,4′-(hexafluoroisopropylidene)diphthalic anhydride (HDA) as the cross-linker.[15] They also demonstrated the fabrication of a hydroxyl-free PVP dielectric layer cross-linked via thiol-end chemistry at 80 °C.[16] However, thermal treatment for over 3 h is still required in their method, which is too time-consuming and inefficient for high throughput manufacturing. In a different approach, Lee et al. reported the preparation of a photocured PVP gate dielectric by using photoacid molecules.[17] After exposure to UV irradiation for 10 min, the photoacid molecules decompose and the PVP film is cross-linked at a temperature of 100 °C for 30 min via the acid catalyzed ring opening polymerization of the cross-linker with epoxy groups. Although optical cross-linking using UV irradiation has been demonstrated for various polymer dielectrics as a low temperature curing method, the processing time is still several tens of minutes.[18,19]

In this study, we demonstrated the instantaneous optical cross-linking of polymer gate dielectrics on a flexible substrate by using intensely pulsed white light (IPWL). An IPWL source, referred to as a flash light, was introduced several years ago as a promising tool for printed electronics.[20] In contrast with conventional heating methods, IPWL can modify structures of nanomaterials in an ambient atmosphere over a large area almost instantaneously—from milliseconds to a few seconds. In addition, it is possible with this method to prevent a thermal damage to the substrate and avoid the complex post-treatment processing usually employed with traditional heating concepts for R2R printing systems.[21,22] Compared to continuous light irradiation, the short pulses of IPLW on the order of micro- and milliseconds can reduced the thermal budget of the sample and enables one to achieve high temperature only in a near-surface region.[23] This is definitely different from a laser technique which is based on the monochromatic light source and focused light spot. IPWL technique based on xenon flash lamp allows large light-spot size which is beneficial to minimize the total number of treatment and provide a swift treatment of large area substance.

Recently, several research groups have demonstrated that IPWL is an efficient optical annealing method for nanomaterials. For example, copper and silver nanoparticles (or nanowires) deposited on plastic substrates have been instantly sintered (or welded) with IPWL irradiation without detriment to the substrates.[20,22,24−27] For polymeric materials, Huang et al. reported that polyaniline nanofibers melt under IPWL irradiation to form a smooth and continuous film from an originally random network of nanofibers.[28] We have also demonstrated that the molecular ordering of conjugated polymers can be effectively controlled by varying the pulse conditions used in IPWL irradiation.[29,30] To the best of our knowledge, there have been no previous reports of the instantaneous cross-linking of polymer gate dielectrics with IPWL irradiation. In this study, less than 2 s irradiation with IPWL of PVP blend films with a common cross-linking agent PMF deposited on a plastic substrate was found to yield fully cured films. We confirmed that the IPWL-cross-linked PVP films have smooth pinhole-free surfaces, as well as low leakage current densities, and good compatibility with organic semiconductors, which means that these films are comparable to PVP thermally cross-linked at 180 °C. A flexible OTFTs based on IPWL-cross-linked PVP was found to exhibit good electrical performance comparable to that of a device with a thermally cross-linked PVP dielectric, as well as a mobility that is retained under mechanical bending deformation. We also confirmed that the preparation of cross-linked PVP dielectrics via IPWL irradiation is scalable to large-area substrates by synchronizing the pulsed light irradiation with the substrate transfer.

2. EXPERIMENTAL SECTION

2.1. Materials. A 200 μm thick poly(ether sulfone) (PES) substrate was purchased from i-Components Co. Heat deflection temperature (@ 1.8 MPa) of PES film provided by the supplier was 195 °C. A 100 μm thick polyethylene terephthalate (PET) substrate was supplied by SKC Co. Poly(3,4-ethylenedioxythiophene):poly(styrenesulfonic acid) (PEDOT:PSS) (Clevios P JET 700 N) was used as received. PVP (M_w = 25 kg mol^{-1}), PMF (M_n = 423 g mol^{-1}), propylene glycol monomethyl ether acetate (PGMEA), 1,2-dichlorobenzene, poly(3-hexylthiophene-2,5-diyl) (P3HT), polystyrene (PS) (M_w = 192 kg mol^{-1}), and pentacene were purchased from Sigma-Aldrich Co.

2.2. Device Fabrication. Each poly(ether sulfone) (PES) substrate was cleaned by performing sonication with ethanol. The substrate was treated with UV-ozone for 5 min. 100 nm PEDOT:PSS was spin-coated onto the PES substrate. The PEDOT:PSS film was then dried at 100 °C for 30 min under ambient conditions. The PVP dielectric film was formed by spin coating a PVP and PMF blend (10:8 w/w) solution in PGMEA at 2000 rpm for 60 s. The deposited film was irradiated with IPWL under ambient conditions. As a reference, a PVP dielectric film was annealed at 180 °C for 1 h in a vacuum oven. Then, 40 nm pentacene was deposited onto the cross-linked PVP layer by thermal evaporation at a rate of 0.1 Å^{-1}. To test the compatibility of the PVP layer with a solution processable organic semiconductor, poly(3-hexylthiophene-2,5-diyl) (P3HT) blended with polystyrene (PS) was prepared with a method described by Lu et al.,[31] a P3HT and PS blend (1:19 w/w) dissolved in 1,2-dichlorobenzene (8 mg/mL) was deposited on cross-linked PVP dielectric by spin-casting at 2000 rpm 60 s. Au source and drain electrodes with a thickness of 100 nm were thermally deposited through a shadow mask. The channel length and width of the device were 100 and 1000 μm, respectively. To measure the capacitance of the cross-linked PVPs, capacitors with metal−insulator−metal configuration were fabricated by depositing top electrode of 100 nm Au. To test the effect of various organic solvents on the capacitance of CPVPs, 0.3 mL of various organic solvents were dropped on the PVP:PMF and CPVPs films and after 5 s the solvents was removed by spinning the substrate at 2000 rpm 60 s using spin coater. The capacitance was measured before and after the organic solvent exposure.

2.3. IPWL Irradiation. A home-built IPWL system combined with a R2R substrate supplier was utilized. The IPWL setup consists of a xenon lamp (PerkinElmer QXF, UK), a power supply unit, capacitors, and a cooling device. The xenon lamp was moved along the *z*-axis. A NOVA II power meter was used to check the light energy. The

DOI: 10.1021/acsami.6b14957
ACS Appl. Mater. Interfaces 2017, 9, 11721−11731

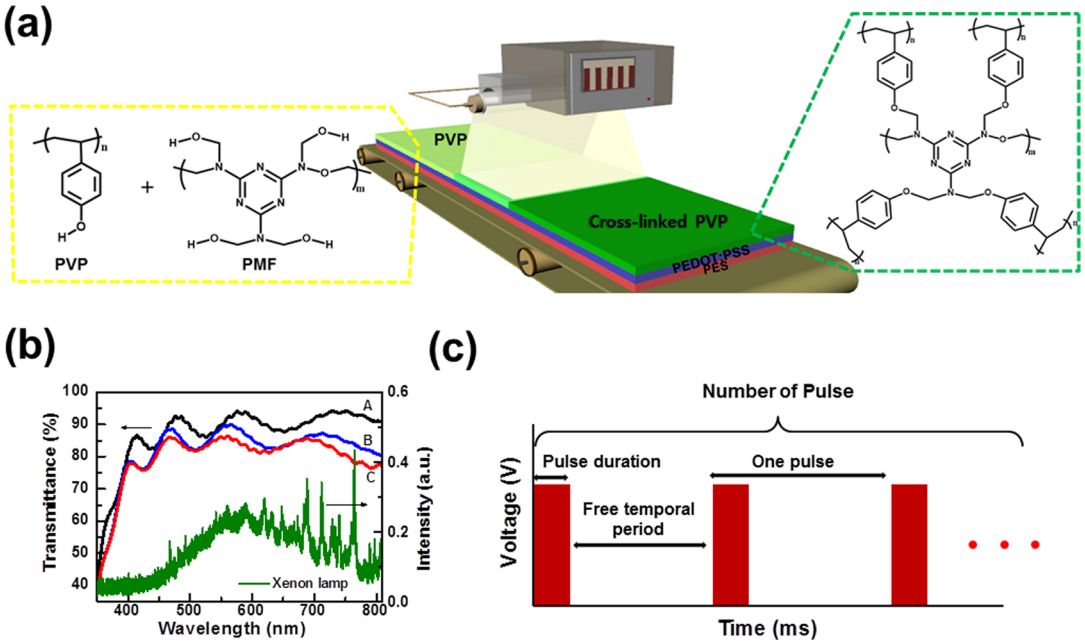

Figure 1. (a) Schematic illustration for cross-linking of poly(4-vinylphenol) (PVP) with poly(melamine-*co*-formaldehyde) (PMF) by using intensely pulsed white light (IPWL). (b) UV−vis transmittance of A:PES, B:PES/PEDOT:PSS(100 nm), C:PES/PEDOT:PSS(100 nm)/PVP(500 nm) and spectra distribution emitted from a xenon flash lamp. (c) Schematic for the pulse parameters of IPWL.

number of pulses was fixed at 50, and the duration and free temporal period were 2 and 10 ms, respectively. The total irradiation energy was controlled from 12.5 to 14.7 J cm^{-2} by varying the applied voltage from 230 to 247 V. For 500 nm thick PVP:PMF film, the irradiation was repeated three times to complete the cross-linking of the PVP and PMF and the total duration time of the irradiation was 1.8 s. In the case of 100 nm thick PVP:PMF film, the irradiation was repeated two times and total duration time of the irradiation was 1.2 s.

2.4. Characterization. The attenuated total reflectance (ATR) transmittance spectra of the film layers were obtained by using a Jasco FT/IR 4200. Thickness of the films were determined using a surface profiler (AlphaStep As-IQ). The morphologies of the PVP dielectric and pentacene layers were analyzed by atomic force microscopy (AFM). 2D grazing-incidence X-ray diffraction (2D GIXD) patterns were obtained at 3C and 6D beamlines of the Pohang Accelerator Laboratory in Korea. The chemical composition of the PVP surface was investigated by using angle resolved X-ray photoelectron spectroscopy (XPS) (PHI 5000 versa Probe, Ulvac-PHI). The electrical properties of the device were characterized at room temperature under ambient conditions using Agilent 1500A and 4284A meters. The field-effect mobilities and threshold voltages of the OTFTs were determined in a saturation regime using a following equation $I_{DS} = ((WC_i)/(2L))\mu(V_{GS} - V_{th})^2$, where C_i is the capacitance of the cross-linked PVP dielectric, and W and L are the channel width and length, respectively. To characterize the deformation stability on the flexible organic transistors, one edge of each substrate was fixed to an armature, and the substrate is bent when the distance of the armature decreases. The device is located at the center of the substrate. When the substrate is much thicker than the deposited thin film, the applied strain in the bending state can be approximated by[32] strain $\cong d_{film}/2R$, where d_{film} is the total thickness of the thin film deposited on the substrate and R is the bending radius.

3. RESULTS AND DISCUSSION

Figure 1a shows a schematic illustration of the procedure for cross-linking PVP with IPWL irradiation. A 500 nm PVP film containing PMF cross-linker (PVP:PMF) was deposited on a PEDOT:PSS coated PES substrate. Conductive PEDOT:PSS thin films were utilized as a bottom gate electrode of the transistor and as a photothermal conversion layer. A possible mechanism for the cross-linking of the PVP:PMF film is discussed below. The IPWL setup consists of a xenon flash lamp, a reflector, a power supply, capacitors, and a pulse controller. The pulse controller triggers the capacitor, which delivers electrical current to the lamp at ms intervals, resulting in the irradiation of the PVP thin film with consecutive light pulses. The xenon lamp emits over a broad spectral range 400−1000 nm (Figure 1b). UV−vis transmittances of PES substrate, PEDOT:PSS (100 nm) coated PES, and PVP:PMF (500 nm) deposited on PEDOT:PSS coated PES were compared to the emission of xenon lamp. PES substrate is transparent in the visible light region with transmittance over 82%. When the PEDOT:PSS was deposited on the PES, 10% addtional absorption of the visible light (@ 600 nm emission maximum of xenon lamp) was observed. After the deposition of PVP:PMF on the PEDOT:PSS coated PES substrate, further 4% increase in visible light absorption was found. In fact, this visible light absorption can induce the heat generation during IPWL irradiation by photothermal conversion effect. (Detailed discussion of possible mechanism for the heat generation by IPWL treatment will be presented later.) The fluence of the irradiation can be controlled by varying the pulse parameters including the pulse duration time, the free temporal period, the applied voltage, and the number of pulses (Figure 1c). In this study, the number of pulses (50), the pulse duration (2 ms), and the free temporal period (10 ms) were fixed, and the irradiation fluence was controlled in the range 12.5−14.7 J cm^{-2} by varying the applied voltage. The PVP:PMF films cross-linked (CPVPs) with IPWL and conventional heating in vacuum (180 °C, 1 h, 10^{-2}−10^{-3} Torr) are referred to as CPVP_IPWL and CPVP_Heat respectively throughout the remainder of the paper.

To optimize the cross-linking density of the PVP:PMF films, FT-IR analysis was performed for different IPWL dosed samples. It was known that the hydroxyl (−OH) groups in PVP are bonded with those in PMF under thermal annealing conditions.[33] As shown in Figure 2a, a strong absorption peak

DOI: 10.1021/acsami.6b14957
ACS Appl. Mater. Interfaces 2017, 9, 11721−11731

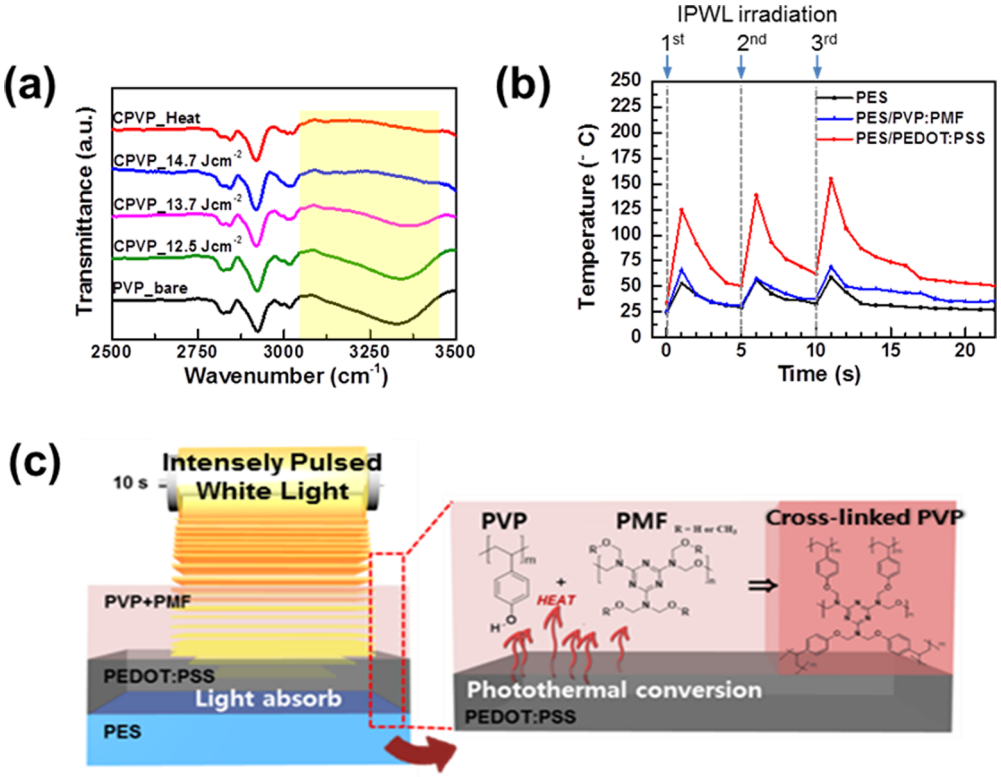

Figure 2. (a) FT-IR spectra of PVP films cross-linked by thermal heating and IPWL irradiation with different light energy. (b) Surface temperatures of the PES substrate, PVP:PMF on PES, and PEDOT:PSS on PES under repeated IPWL three times with 5 s intervals. (c) Expected mechanism of cross-linking PVP and PMF by photothermal effect arised from PEDOT:PSS layer under IPWL irradiation.

due to −OH groups in the as-prepared PVP:PMF film was observed at 3000−3450 cm^{-1}. After thermal cross-linking at 180 °C for 1 h in vacuum, the −OH related peak has almost disappeared. Interestingly, when the PVP:PMF film was briefly exposed to IPWL with a light energy of 14 Jcm^{-2} for 1.8 s, the −OH related peak was also significantly diminished, which indicates that PVP:PMF is successfully cross-linked by irradiation with IPWL. After the IPWL cross-linking, there was no thermal damage to the PES supporting substrate, such as distortion or burn mask. We also found that the IPWL irradiation energy affect the degree of cross-linking. When the IPWL energy is below 14 J cm^{-2}, unreacted hydroxyl groups are still evident in the FT-IR spectrum, indicating that cross-linking is not complete. Whereas the distortion of the PES substrate was observed after exposure of high intensity light. IPWL irradiation time can be related to the film thickness. When the thinner PVP:PMF film with 100 nm thickness were demonstrated, IPWL irradiation for 1.2 s was enough to cross-link the film (see Supporting Information (SI) Figure S1). The degree of cross-linking in PVP:PMF films by varying mixing ratio of PVP and PMF was referentially investigated (see SI Figure S2). FT-IR spectra exhibited that 10:8 w/w ratio PVP:PMF showed the minimized −OH absorption peak under the constant irradiation condition, indicating the cross-linking density might be maximized at the PVP:PMF mixting ratio. Based on this result, remainder characterizations for CPVPs including the surface and electrical properties and the fabrication of the OTFT devices were performed using the 10:8 w/w ratio PVP:PMF composition.

To provoke chemical reaction between PVP and PMF molecules, the IPWL irradiation needs to provide a certain amount of heat to the PVP:PMF film because specific photoinitiators or catalysts for reaction initiation were not utilized in this study. To understand thermal cross-linking reaction, differential scanning calorimeter (DSC) thermograms for PVP, PMF, and PVP:PMF mixture were compared in SI Figure S3. (Detailed explanation for thermal gravimetric analysis (TGA) of each of the components will be presented in SI Figure S4) Multiple endothermic peaks shown in PVP:PMF mixture at the temperature range of 135−158 °C could be attributed to heat absorbed in sudden phase change of PMF or when the small molecules such as water or methanol formed by cross-linking were liberated.[34] Even though exothermic peaks evolved in the cross-linking reaction was not clearly shown due to strong endothermic peaks of PMF molecules, we found that the cross-linking reaction was completed in the temperature range about 130−180 °C because no more noticeable peaks were observed in further cooling and second heating process. Additionally, the characteristic glass transition temperature of PVP (186 °C) was not observed in thermogram of PVP:PMF mixture. Based on these results, we can reasonably infer that temperature increase above 130 °C is required to induce the cross-linking reaction in PVP:PMF mixture during IPWL irradiation. It has been reported that the consecutive intensely pulsed light (or flash light) irradiation of nanomaterials such as carbon nanotubes, conducting polymer nanoparticles, and silicon nanowires generates heat that instantly increases the material temperature above 1000 °C.[28,35−37] Although the mechanism for this instant temperature increase is not yet fully understood, photothermal conversion, in which thermal energy is released by light-absorbing agents, is believed to be the primary cause.[28,38]

To verify direct heat generation during the IPWL treatment, the surface temperature of the sample was monitored with a

DOI: 10.1021/acsami.6b14957
ACS Appl. Mater. Interfaces 2017, 9, 11721−11731

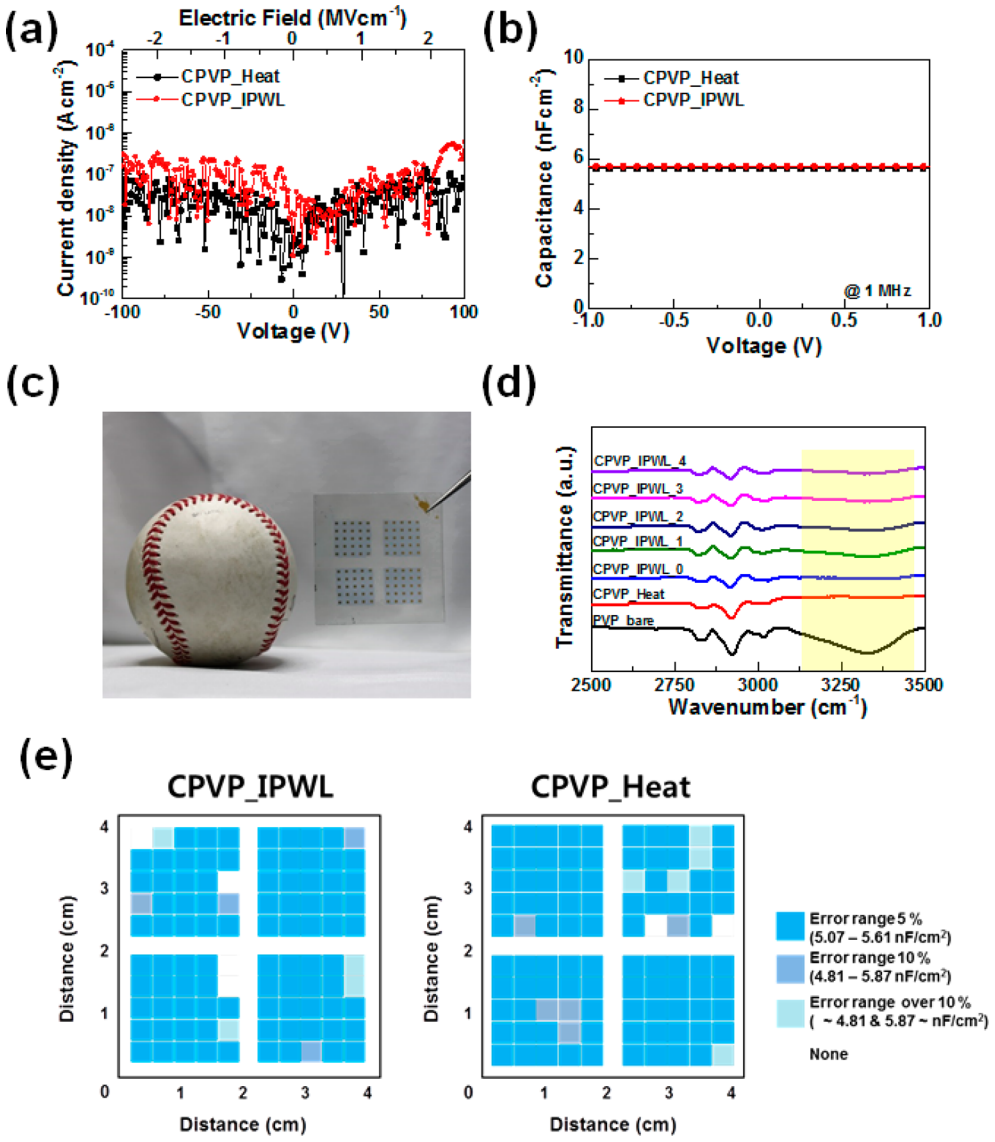

Figure 3. (a) Current density versus voltage (or electric field) plot for CPVP_Heat and CPVP_IPWL dielectrics. (b) Capacitance values for CPVP_Heat and CPVP_IPWL dielectrics. (c) Photograph of 5 × 5 cm^2 area CPVP_IPWL coated sample. (d) FT-IR spectra of CPVP_IPWL film at different 5 positions with an interval of 1 cm. (e) Comparison in capacitance distribution of CPVP_IPWL and CPVP_Heat films measured at 100 different positions over 5 × 5 cm^2 area.

digital thermocouple. The thermocouple probes were attached to the perimeter of the sample and covered with a light blocking layer because direct exposure of the thermocouple probe to IPWL would increase the temperature of the probe (see SI Figure S5). Note that the surface temperature is certainly underestimated by the thermocouple measurements because of the detection limit of the thermocouple (1 s) and heat losses between the IPWL-exposed area and the thermocouple probe. Figure 2b compares the surface temperatures of the PES supporting substrate, PVP:PMF on PES, and PEDOT:PSS on PES after IPWL irradiation with a light intensity of 14 J cm^{-2} repeated three times. Notably, a light-exposure time of a one-off IPWL irradiation was only 0.6 s and irradiation was repeated with an interval of 5 s to charge a capacitor. When only the PVP:PMF film is present on the PES substrate, only a small increase in the surface temperature was observed during IPWL irradiation. However, for PEDOT:PSS on PES, the surface temperature was dramatically increased up to almost 150 °C. This temperature is below the heat deflection temperature of PES substrate (195 °C). However, when the light intensity of IPWL was increased further, the distortion of the substrate was observed, as mentioned above. This indicates that higher temperature than the heat deflection temperature of the PES substrate can be reached by IPWL irradiation. It has previously been reported that conjugated polymers such as PEDOT:PSS are good at converting light energy into heat energy.[38] This result indicates intensely pulsed visible light emitted from the flash lamp is preferentially absorbed by the PEDOT:PSS layer and instantly releases the heat energy via photothermal conversion, which provides sufficient energy to provoke the cross-linking reaction in PVP and PMF. Additionally, it can be anticipated that the residual PGMEA solvent (b.p 145 °C) and possible byproducts (H_2O or methanol) formed in cross-linking reaction might be evaporated due to the instantly increased temperature. The possible mechanism for PVP cross-linked by IPWL irradiation was illustrated in Figure 2c.

In order to compare the dielectric properties of the CPVPs obtained with the two cross-linking methods, the leakage

DOI: 10.1021/acsami.6b14957
ACS Appl. Mater. Interfaces 2017, 9, 11721−11731

current densities of capacitors based on the CPVPs were measured. The breakdown voltage of a dielectric is the voltage that it can endure as an insulator until current flows. Figure 3a shows that CPVP_IPWL does not undergo dielectric breakdown until 2.0 MVcm^{-1}, as is the case for CPVP_Heat. The leakage current density of CPVP_IPWL is below 3×10^{-7} Acm^{-2} at 80 V, which is close to the leakage currents of thermally grown SiO_2 dielectrics.[8] Without the cross-linking, capacitance of PVP is about 4.8 nFcm^{-2}. In comparison, the average capacitance of CPVP_IPWL is 5.7 nFcm^{-2}, which is almost identical to that of CPVP_Heat within a standard deviation of ±10% (Figure 3b). The increased capacitances of the CPVPs compared to non-cross-linked PVP are related to the decrease of the film thickness after cross-linking reaction, where the thickness of PVP:PMF decreased from 600 to 500 nm after cross-linking (see SI Figure S6). It was found that there was no difference in the film thickness variation according to different cross-linking methods. The use of IPWL irradiation could be particularly beneficial in high throughput large area roll-to-roll processes. To test the feasibility of the IPWL cross-linking of PVP dielectrics for large area manufacturing, the cross-linking of PVP:PMF films deposited on 5×5 cm^2 PES substrates was demonstrated (Figure 3c). Although the length and width of the xenon flash lamp are approximately 5 and 1 cm respectively, the home-built IPWL setup with its roll-to-roll feeding unit enables the transfer of the substrate at constant speed during IPWL irradiation. A movie for IPWL irradiation on the large area substrate was provided in SI. The FT-IR spectra of CPVP_IPWL on a large area substrate recorded for five different positions at an interval of 1 cm indicate that the synchronization of continuous IPWL irradiation with the transfer of the substrate enables the uniform cross-linking of PVP:PMF over a large area (Figure 3d). To investigate the cross-linking uniformity of CPVP_IPWL, its capacitance was measured at 100 different positions over a 5×5 cm^2 area. As shown in Figure 3e, the capacitance values of CPVP_IPWL measured at 89 positions are almost identical within 5% error, which is comparable to the results obtained for CPVP_Heat. This result shows that this method for the preparation of cross-linked PVP dielectric layers is compatible to high throughput large area processes because of the successful implementation of the IPWL irradiation system.

The surface properties of gate dielectrics affect the molecular orientations and morphologies of organic semiconductor thin films, which determine the electrical properties of organic transistors. Figure 4a and b show topological images of CPVPs obtained with atomic force microscopy (AFM). CPVP_IPWL has a smooth pinhole-free surface with a root-mean square (RMS) roughness of 0.321 nm, which is comparable to that of CPVP_Heat (0.383 nm). The morphologies of pentacene thin films vacuum-deposited on the CPVP dielectrics were investigated. Typical terrace-like structures with sizes ranging from 160 to 400 nm was observed on the pentacene film grown on CPVP_Heat (Figure 4c). In contrast, larger pentacene grains with sizes above 1 μm were found on CPVP_IPWL (Figure 4d). Since the surface roughnesses of these PVP films are almost identical, this difference can be mainly attributed to the different surface energies of the CPVP dielectrics that arise with the different cross-linking method. It is known that when the surface roughness is negligible, pentacene growth tends to shift from the large terrace-structured grains produced by the Stranski-Krastanov mode to the small three-dimensional grains of the Volmer−Weber growth mode, as the surface energy of

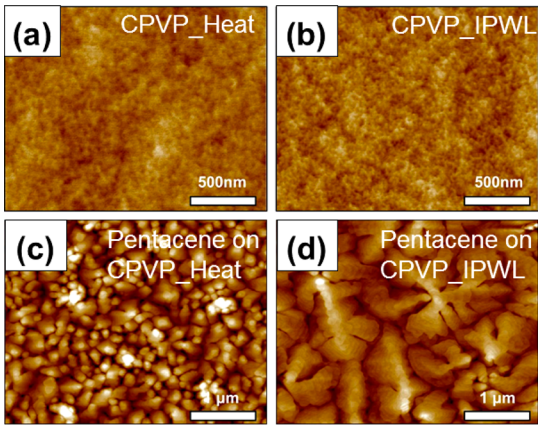

Figure 4. AFM topographies of the cross-linked PVP films by using (a) thermal heating and (b) IPWL irradiation. AFM images of the 25 nm pentacene films deposited on (c) CPVP_Heat and (d) CPVP_IPWL dielectrics.

the dielectric layer decreases.[39,40] In fact, our surface energy estimates obtained with contact angle measurements confirm that CPVP_IPWL has a higher surface energy (51.7 mJ/m^2) than CPVP_Heat (37.7 mJ/m^2) (see SI Figure S7). To investigate the origin of the differences in surface energy between CPVP_IPWL and CPVP_Heat, the chemical compositions of the film surfaces were analyzed by recording angle resolved X-ray photoemission spectra (Figure 5, Table 1). For CPVP_Heat, the atomic ratio of N 1s, which originates from the PMF cross-linker, to C 1s is independent of the takeoff angle. In contrast, a high N 1s/C 1s value at low takeoff angles was obtained for the CPVP_IPWL film. This result means that the concentration of polar PMF molecules is higher at the surface of the CPVP_IPWL film than for CPVP_Heat. When PVP:PMF films are cross-linked in vacuum at a high temperature, a considerable quantity of unreacted PMF molecules can evaporate.[41] In contrast, during cross-linking with IPWL irradiation under ambient conditions, most PMF molecules are expected to remain in the film. The higher PMF content at the surface of CPVP_IPWL when compared to the bulk of the film is attributed to the migration of the PMF molecules near the underlying PEDOT:PSS layer toward the film surface due to the rapid increase in the temperature that arises from the photothermal conversion in the PEDOT:PSS during IPWL irradiation. This high concentration of PMF molecules at the surface of the CPVP_IPWL film substantially increases the polar interaction component of the surface energy (see SI Figure S7). In addition, the surface oxidation effect by the activated oxygen in the air, which can be generated when the high energy light irradiates on the substance in the ambient condition, need to be also considered. We compared the chemical compositions of CPVP_Heat at the surface before and after the IPWL irradiation (see SI Figure S8). As a result, almost no variation in the intensity ratio of C−O to C−C was observed, indicating that surface oxidation effect by IPWL is negligible.

In addition, the crystalline natures of the pentacene molecules deposited on the CPVP_IPWL and CPVP_Heat dielectrics were characterized by using two-dimensional grazing incident angle X-ray diffraction (2D GIXD) (see SI Figure S9). For both CPVP dielectrics, the strong reflection along the q_z axis with a layer spacing of 15.1−15.4 Å indicates the presence of (001) crystalline planes. The Bragg rods along the substrate

DOI: 10.1021/acsami.6b14957
ACS Appl. Mater. Interfaces 2017, 9, 11721−11731

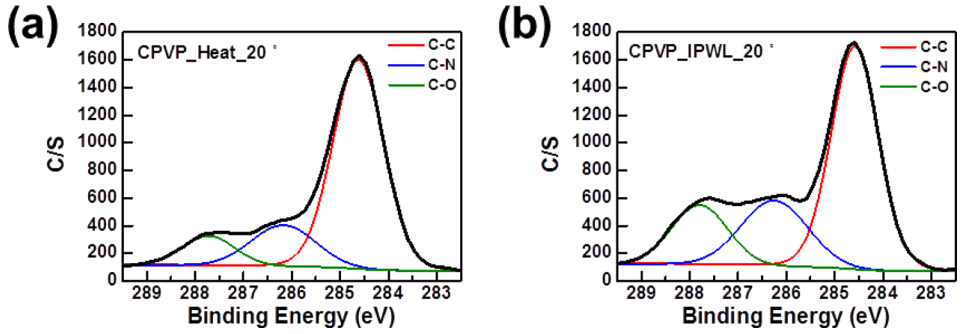

Figure 5. C 1s X-ray photoemission spectroscopy (XPS) spectra obtained at the takeoff angle of 20° for differently cross-linked PVP films; (a) CPVP_Heat and (b) CPVP_IPWL. The takeoff angle dependent atomic ratio N/C was summarized below the XPS spectra.

Table 1. Take-off Angle Dependent Atomic Ratio N/C Was Summarized Below the XPS Spectra

N/C intensity ratio	20°	50°	90°
CPVP_Heat	0.24	0.29	0.29
CPVP_IPWL	0.43	0.37	0.34

normal at fixed q_{xy} positions indicate that the pentacene molecules are three-dimensionally well-stacked on the surfaces of the CPVP dielectrics. Both 2D GIXD patterns provide clear evidence of a thin film phase with $d_{(001)}$ = 15.4 Å and no bulk phase structure with smaller layer spacing is evident. In contrast to the morphological differences found between the pentacene films grown on CPVP_IPWL and CPVP_Heat, as shown in Figure 4c and d, the crystalline natures of the pentacene layers are almost identical. As discussed below, the similarity of the crystalline structures of the pentacene layers grown on CPVP_IPWL and CPVP_Heat means that they exhibit almost identical charge carrier mobilities in field-effect transistors. Further investigations of the nucleation and growth mechanism of pentacene molecules on the CPVP_IPWL dielectric have been performed. In particular, the crystalline morphologies and structures of first few monolayers on the dielectric surfaces is important because the charge carrier transport in pentacence transistor mainly takes place at the semiconductor/dielectric interfaces.[42,43] Comprehensive studies including the effect of pentacene deposition rate and substrate temperature on the early stage crystalline structure, and its relation to charge carrier mobility and charge trap behaviors of the device will be carried out.

To verify the organic solvent resistance of the CPVP_IPWL dielectric for the compatibility of solution processable organic semiconductors, the capacitance change of the CPVPs by exposure of various organic solvents was investigated (Figure 6). Acetone, isopropyl alcohol (IPA), and PGMEA were selected as a good solvent for PVP and chlorinated solvents such as chloroform (CF), chlorobenzene (CB), dichlorobenzene (DCB) were used as a poor solvent for PVP. Without cross-linking reaction, PVP:PMF film was removed by exposure of good solvents. For the chlorinated poor solvents the PVP:PMF did not dissolved, but from 5 to 10% variations in capacitance were observed. By contrast, cross-linked PVPs were not removed even when the good solvents were casted, and thickness changes in the cross-linked PVPs was not detected. In particular, CPVP_IPWL exhibited small variations in capacitance change after the organic solvents exposure, which was comparable to the capacitance change of the CPVP_Heat. Somewhat larger capacitance change in CPVP_IPWL compared to that in CPVP_Heat, when the good solvent was casted, might be due to enhanced polar interaction component of CPVP_IPWL surface which can strongly attract the polar solvent molecules. This result strongly supports that PVP cross-linked with IPWL irradiation has sufficient organic−solvent resistance.

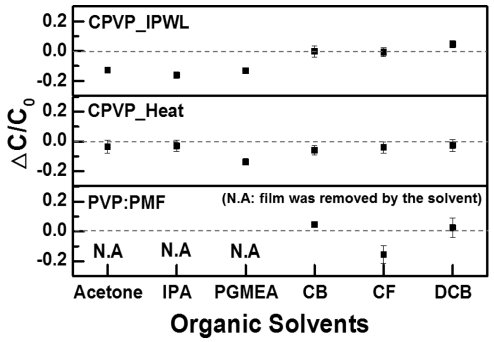

Figure 6. Capacitance change of CPVP_IPWL, CPVP_Heat and PVP films after exposure to various organic solvents; acetone, isopropyl alcohol (IPA), propylene glycol monomethyl ether acetate (PGMEA), chlorobenzene (CB), chloroform (CF), and dichlorobenzene (DCB).

Figure 7a and b show the transfer characteristics of the pentacene transistors based on the CPVPs cross-linked via thermal heating and IPWL irradiation. The device characteristics, including the field-effect mobility, the on/off ratio, the threshold voltage, and the subthreshold swing, are summarized in Table 2. The average field-effect mobility and on/off current ratio of the transistor with the CPVP_IPWL dielectric are 0.23 $cm^2V^{-1}s^{-1}$ and about $\sim 10^5$ respectively, and a low leakage current level of 10^{-9} A and no hysteresis were observed. These values are comparable to that of the device with the CPVP_Heat dielectric, which is attributed to the similar properties of the dielectrics and the molecular orientation of the pentacene molecules, as mentioned above. To confirm the compaibility of the CPVP_IPWL dielectric with the solution processed organic semiconductor, P3HT transistors were fabricated by spin coating of P3HT on the CPVP_IPWL dielectric (see SI Figure S10). The carrier mobility and on/off current ratio of the P3HT transistor with CPVP_IPWL are 0.03 $cm^2V^{-1}s^{-1}$ and 10^4 respectively, as are those of the device with a typical CPVP_Heat dielectric. This result confirmed that the CPVP_IPWL is compatible with the solution processed organic semiconductors. In addition, to test the feasibility of the IPWL cross-linking of PVP to the low-cost plastic substrates, the P3HT transistors were fabricated using CPVPs deposited on a polyethylene terephthalate (PET) substrate (see SI Figure

DOI: 10.1021/acsami.6b14957
ACS Appl. Mater. Interfaces 2017, 9, 11721−11731

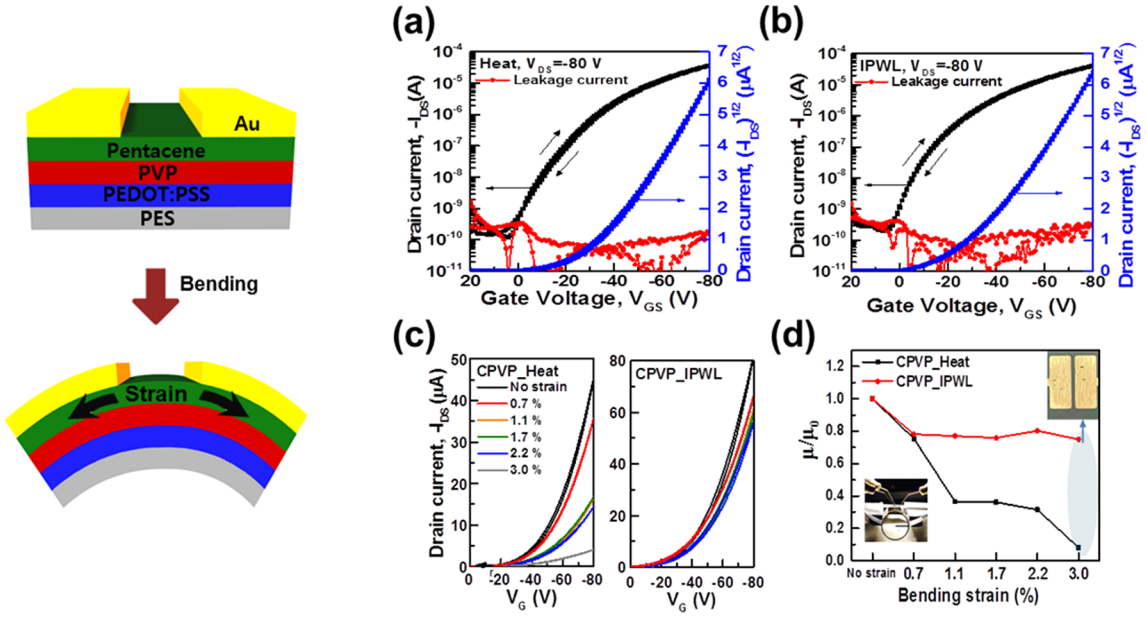

Figure 7. Schematic configuration of the flexible organic transistors based on cross-linked PVP dielectric and pentacene active layer was displayed on the left. Transfer characteristics ($I_{DS} - V_{GS}$) of the pentacene transistors with differently cross-linked PVP dielectrics; (a) CPVP_Heat and (b) CPVP_IPWL. The variation in (c) the transfer characteristics and (d) field-effect mobilities of the flexible pentacene transistors with differently cross-linked CPVP films as a function of tensile bending strain.

Table 2. Properties of Pentacene Devices with PVP Insulators Treated by Heat or IPWL

	electrical parameters			
gate dielectric	μ^{avg} ($cm^2V^{-1}s^{-1}$)	$I_{on}/I_{off}{}^{avg}$	$V_{th}{}^{avg}$ (V)	SS^{avg} ($Vdec^{-1}$)
CPVP_Heat	0.24 (±0.04)	9.6×10^4	−25 (±0.8)	−8.3 (±2.4)
CPVP_IPWL	0.23 (±0.06)	7.0×10^4	−22 (±2.3)	−7.3 (±3.1)

S11). Compared to the PES substrate, PET substrate can be easily deform during the thermal treatment process due to low glass transition temperature (about 70 °C) and high thermal expansion coefficient. In fact, when the PVP:PMF deposited on PET substrate was thermally cross-linked, the substrate was considerably bent. However, in the case of IPWL cross-linking, although a slight bending of the substrate was observed, the degree of distortion was not severe compared to the thermally cross-linked sample. P3HT transistors based on the thermally cross-linked PVP exhibited high gate leakage current and poor charge carrier mobility. By contrast, the device with CPVP_IPWL on PET substrate showed lower gate leakage current and improved charge carrier mobility compared to the device with CPVP_Heat on PET. This result confirmed that IPWL cross-linking method can be more applicable to the low-temperature processable plastic substrates.

The effects of bending strain on the operation of the flexible organic transistors incorporating cross-linked PVP gate dielectrics were determined. The electrical properties of the devices were evaluated at various tensile strains in the range 0–3% (bending radii down to 3 mm). As shown in Figure 7c and d, the mobility of the device with the CPVP_Heat dielectric dramatically decreases due to a significant reduction in the on-current with increases in the bending strain, whereas the device with CPVP_IPWL exhibits only a small decrease in the on-current, and the mobility retained more than 75% of its original value even when the bending strain increases up to 3%. The drastic deterioration in the performances of both devices at a bending strain of 3% is due to the cracking of the top gold source and drain electrodes, as shown in the inset in Figure 7d. Several fundamental studies of flexible organic transistors have reported that the molecular structures and film morphologies of organic semiconductors and the surface properties of polymer gate dielectrics are related to the electrical properties of OTFTs in the presence of strain.[32,44−47] In general, charge transport in pentacene is closely related to the charge hopping rate, and the charge carrier mobility tends to decrease under tensile strain due to the larger spacing between the pentacene molecules.[32,47] More recently, Sokolov et al. also demonstrated that the strain-induced rearrangement of the polymer chains at the dielectric surface affects the charge transport at the semiconductor/dielectric surface interface.[46] In that study, a pentacene transistor with a thermally cross-linked PVP dielectric was found to exhibit an unexpectedly large change in its mobility under applied strain even though the polymer chain movement in the cross-linked PVP was limited; the heterogeneity arising from the presence of the cross-linker in the polymer matrix was considered a principal cause of this reduction in mobility. The origin of the improved bending stability of the device with the CPVP_IPWL dielectric needs to be investigated further, but the more homogeneous distribution of PMF cross-linker molecules at the surface of the CPVP_IPWL dielectric gives rise to its homogeneous surface potential. As mentioned above, PMF molecules are readily evaporated during the thermal cross-linking process, so cross-linking reaction sites at the film surface might be relatively scarce and thus surface potential variation upon mechanical strain could be induced by chain rearrangement. In contrast, a substantial number of PMF

DOI: 10.1021/acsami.6b14957
ACS Appl. Mater. Interfaces 2017, 9, 11721−11731

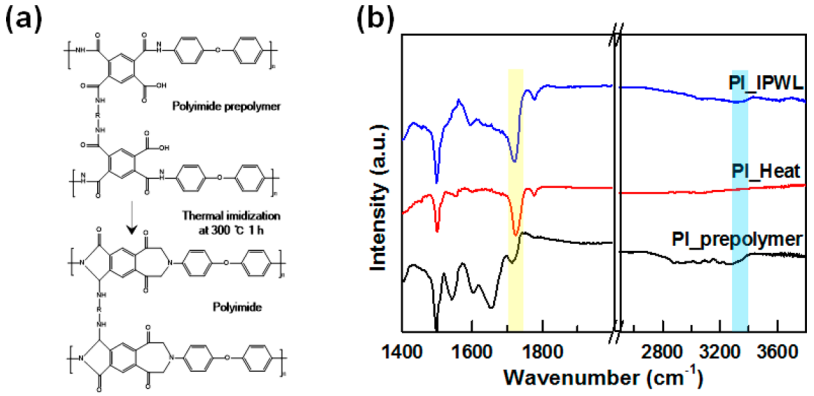

Figure 8. (a) Chemical reactions in the imidization of poly(amic acid) prepolymer and (b) FT-IR spectra of PI_Heat cured at 300 °C 1h, and PI_IPWL with IPWL irradiation for approximately 10 s.

molecules remain in the film after cross-linking with IPWL irradiation, so dense cross-linking at the film surface is likely to limit chain movement in the presence of strain.

Although this study focused on PVP dielectrics, the chemical reactions induced by IPWL irradiation can probably be applied to other cross-linked polymer systems such as polyimide, epoxy resins, poly(vinyl alcohol), etc. As a preliminary test, we confirmed that a polyimide can be simply prepared by exposing the poly(amic acid) prepolymer film to IPWL irradiation; such imidization reactions are generally performed by thermal heating at high temperatures above 300 °C (Figure 8a).[48] FT-IR spectra of polyimide films cross-linked with thermal heating (PI_Heat) at 300 °C 1 h, and with IPWL irradiation (PI_IPWL) for approximately 10 s are shown in Figure 8b. After the imidization reaction, the absorption peaks at 1724 cm^{-1} and 3428−3352 cm^{-1}, related to symmetrical stretching of imide and amines of polyimide prepolymer, respectively.[49]

4. CONCLUSIONS

The instantaneous cross-linking of a polymer dielectric on a flexible substrate by using intensely pulsed white light irradiation was demonstrated. Less than 2 s of IPWL irradiation of PVP:PMF films deposited on a plastic substrate yielded fully cross-linked dielectric layers. Various characterizations were performed to confirm that the PVP films cross-linked with IPWL irradiation have smooth pinhole-free surfaces and exhibit low leakage current densities below 10^{-7} Acm^{-2}, as well as organic-solvent resistance. These characteristics mean that these dielectrics can be used as replacements for thermally cross-linked PVP dielectrics. We considered the possible mechanism of the IPWL-induced cross-linking of PVP, and suggested that the photothermal conversion of the PEDOT:PSS underlayer utilized as a gate electrode for the flexible TFT might provide sufficient heat to induce the cross-linking reaction between the PVP and PMF molecules. The synchronization of the IPWL irradiation with substrate transfer was tested and found to enable the cross-linking of large-area PVP films, which then exhibit highly uniform capacitance. A flexible OTFT based on IPWL-cross-linked PVP was found to exhibit good electrical performance that is comparable to that of the device with a thermally cross-linked PVP dielectric, and its mobility retained more than 75% of its original value when the bending strain increases up to 3%. We believe that the proposed concept of IPWL-driven cross-linking of polymer dielectrics can be extended to various materials that require low temperature processing and high speed chemical modification.

■ ASSOCIATED CONTENT

Supporting Information

The Supporting Information is available free of charge on the ACS Publications website at DOI: 10.1021/acsami.6b14957.

FT-IR spectra of 100 nm PVP:PMF films cross-linked by thermal heating and IPWL irradiation with 14 J cm^{-2}. FT-IR spectra of PVP:PMF films with various mixing ratio after exposure of IPWL irradiation. Differential scanning calorimertry (DSC) thermograms of PVP, PMF and mixture of PVP:PMF (10:8 w/w ratio) solution. Thermal gravimetric analysis (TGA) of PVP, PMF and PVP:PMF mixture. Scheme for the in situ measurement of the surface temperature of the film during IPWL irradiation. Height profiles showing the changes in the thickness of PVP films before and after cross-linking using thermal annealing and IPWL irradiation. Surface energy analysis of CPVP_Heat and CPVP_IPWL dielectrics by using contact angle measurement. X-ray photoemission spectra obtained at the takeoff angle 15° for CPVP_Heat and CPVP_Heat with IPWL irradiation. 2D GIXD patterns of 25 nm-thick pentacene films on CPVP_Heat and CPVP_IPWL. Transfer characteristics (I_{DS}−V_{GS}) and output characteristics (I_{DS}-V_{DS}) of the P3HT-based transistors with cross-linked PVP dielectrics. Transfer characteristics (I_{DS}−V_{GS}) and output characteristics (I_{DS}−V_{DS}) of the P3HT-based transistors using PET substrate coated with cross-linked PVP (PDF)
(AVI)

■ AUTHOR INFORMATION

Corresponding Authors

*(H.Y.) Phone: +82-32-860-7494; e-mail: hcyang@inha.ac.kr.
*(J.A.L.) Phone: +82-2-958-5378; e-mail: jalim@kist.re.kr.

ORCID

Hoichang Yang: 0000-0003-0585-8527
Jung Ah Lim: 0000-0002-3007-3855

Notes

The authors declare no competing financial interest.

■ ACKNOWLEDGMENTS

This study was supported by the Future Resource Research Program of the Korea Institute of Science and Technology (KIST) (2E26390) and the Industrial Fundamental Technol-

ogy Development Program (10051440) funded by the Ministry of Trade, Industry and Energy (MOTIE), Korea. This work was supported by the National Research Foundation of Korea (NRF) grant funded by the Ministry of Science, ICT & Future Planning (MSIP) (2015R1A2A1A01004354).

REFERENCES

(1) Baude, P. F.; Ender, D. A.; Haase, M. A.; Kelley, T. W.; Muyres, D. V.; Theiss, S. D. Pentacene-Based Radio-Frequency Identification Circuitry. *Appl. Phys. Lett.* **2003**, *82*, 3964−3966.
(2) Noda, M.; Kobayashi, N.; Katsuhara, M.; Yumoto, A.; Ushikura, S.; Yasuda, R.; Hirai, N.; Yukawa, G.; Yagi, I.; Nomoto, K.; Urabe, T. An OTFT-Driven Rollable OLED Display. *J. Soc. Inf. Disp.* **2011**, *19*, 316−322.
(3) Lin, P.; Yan, F. Organic Thin-Film Transistors for Chemical and Biological Sensing. *Adv. Mater.* **2012**, *24*, 34−51.
(4) Brown, A. R.; Pomp, A.; Hart, C. M.; de Leeuw, D. M. Logic Gates Made from Polymer Transistors and Their Use in Ring Oscillators. *Science* **1995**, *270*, 972−974.
(5) Minemawari, H.; Yamada, T.; Matsui1, H.; Tsutsumi, J.; Haas, S.; Chiba, R.; Kumai, R.; Hasegawa, T. Inkjet Printing of Single-Crystal Films. *Nature* **2011**, *475*, 364−367.
(6) Mitsui, C.; Okamoto, T.; Yamagishi, M.; Tsurumi, J.; Yoshimoto, K.; Nakahara, K.; Soeda, J.; Hirose, Y.; Sato, H.; Yamano, A.; Uemura, T.; Takeya, J. High-Performance Solution-Processable N-Shaped Organic Semiconducting Materials with Stabilized Crystal Phase. *Adv. Mater.* **2014**, *26*, 4546−4551.
(7) Briseno, A. L.; Tseng, R. J.; Ling, M.-M.; Falcao, E. H. L.; Yang, Y.; Wudl, F.; Bao, Z. High-Performance Organic Single-Crystal Transistors on Flexible Substrates. *Adv. Mater.* **2006**, *18*, 2320−2324.
(8) Klauk, H.; Halik, M.; Zschieschang, U.; Schmid, G.; Radlik, W.; Weber, W. High-Mobility Polymer Gate Dielectric Pentacene Thin-Film Transistors. *J. Appl. Phys.* **2002**, *92*, 5259−5263.
(9) Lim, M.-H.; Jung, W.-S.; Park, J.-H. Curing Temperature-and Concentration-Dependent Dielectric Properties of Cross-linked Poly-4-vinylphenol (PVP). *Curr. Appl. Phys.* **2013**, *13*, 1554−1557.
(10) Halik, M.; Klauk, H.; Zschieschang, U.; Schmid, G.; Radlik, W.; Weber, W. Polymer Gate Dielectrics and Conducting-Polymer Contactsfor High-Performance Organic Thin-Film Transistors. *Adv. Mater.* **2002**, *14*, 1717−1722.
(11) Yang, S. Y.; Kim, S. H.; Shin, K.; Jeon, H.; Park, C. E. Low-Voltage Pentacene Field-Effect Transistors with Ultrathin Polymer Gate Dielectrics. *Appl. Phys. Lett.* **2006**, *88*, 173507.
(12) Chen, F.-C.; Chu, C.-W.; He, J.; Yang, Y.; Lin, J.-L. Organic Thin-Film Transistors With Nanocomposite Dielectric Gate Insulator. *Appl. Phys. Lett.* **2004**, *85*, 3295−3297.
(13) Kim, J.; Lim, S. H.; Kim, Y. S. Solution-Based TiO_2−Polymer Composite Dielectric for Low Operating Voltage OTFTs. *J. Am. Chem. Soc.* **2010**, *132*, 14721−14723.
(14) Chen, F.-C.; Chuang, C.-S.; Lin, Y.-S.; Kung, L.-J.; Chen, T.-H.; Shieh, H.-P. D. Low-Voltage Organic Thin-Film Transistors with Polymeric Nanocomposite Dielectrics. *Org. Electron.* **2006**, *7*, 435−439.
(15) Roberts, M. E.; Queraltó, N.; Mannsfeld, S. C. B.; Reinecke, B. N.; Knoll, W.; Bao, Z. Cross-Linked Polymer Gate Dielectric Films for Low-Voltage Organic Transistors. *Chem. Mater.* **2009**, *21*, 2292−2299.
(16) Wang, C.; Lee, W.-Y.; Nakajima, R.; Mei, J.; Kim, D. H.; Bao, Z. Thiol−ene Cross-Linked Polymer Gate Dielectrics for Low-Voltage Organic Thin-Film Transistors. *Chem. Mater.* **2013**, *25*, 4806−4812.
(17) Lee, T. W.; Shin, J. H.; Kang, I. N.; Lee, S. Y. Photocurable Organic Gate Insulator for the Fabrication of High-Field Effect Mobility Organic Transistors by Low Temperature and Solution Processing. *Adv. Mater.* **2007**, *19*, 2702−2706.
(18) Jang, J.; Kim, S. H.; Hwang, J.; Nam, S.; Yang, C.; Chung, D. S.; Park, C. E. Photopatternable Ultrathin Gate Dielectrics for Low-Voltage-Operating Organic Circuits. *Appl. Phys. Lett.* **2009**, *95*, 073302.
(19) Pyo, S. H.; Lee, M. Y.; Jeon, J. J.; Lee, J. H.; Yi, M. H.; Kim, J. S. An Organic Thin-Film Transistor with a Photoinitiator-Free Photosensitive Polyimide as Gate Insulator. *Adv. Funct. Mater.* **2005**, *15*, 619−626.
(20) Kim, H.-S.; Dhage, S. R.; Shim, D.-E.; Hahn, H. T. Intense Pulsed Light Sintering of Copper Nanoink for Printed Electronics. *Appl. Phys. A: Mater. Sci. Process.* **2009**, *97*, 791−798.
(21) Hosel, M.; Krebs, F. C. Large-Scale Roll-to-Roll Photonic Sintering of Flexo Printed Silver Nanoparticle Electrodes. *J. Mater. Chem.* **2012**, *22*, 15683−15688.
(22) Helgesen, M.; Carle, J. E.; Andreasen, B.; Hosel, M.; Norrman, K.; Sondergaard, R.; Krebs, F. C. Rapid Flash Annealing of Thermally Reactive Copolymers in a Roll-to-Roll Process for Polymer Solar Cells. *Polym. Chem.* **2012**, *3*, 2649−2655.
(23) Gebel, T.; Rebohle, L.; Fendler, R.; Hentsch, W.; Skorupa, W.; Voelskow, M.; Anwand, W.; Yankov, R. A. In Millisecond Annealing with Flashlamps: Tool and Process Challenges. *Int. Conf. Adv. Therm. Process. Semicond.* **2006**, *14*, 47−55.
(24) Kang, J. S.; Ryu, J.; Kim, H. S.; Hahn, H. T. Sintering of Inkjet-Printed Silver Nanoparticles at Room Temperature Using Intense Pulsed Light. *J. Electron. Mater.* **2011**, *40*, 2268−2277.
(25) Kang, H.; Sowade, E.; Baumann, R. R. Direct Intense Pulsed Light Sintering of Inkjet-Printed Copper Oxide Layers Within Six Milliseconds. *ACS Appl. Mater. Interfaces* **2014**, *6*, 1682−1687.
(26) Rager, M. S.; Aytug, T.; Veith, G. M.; Joshi, P. Low-Thermal-Budget Photonic Processing of Highly Conductive Cu Interconnects Based on CuO Nanoinks: Potential for Flexible Printed Electronics. *ACS Appl. Mater. Interfaces* **2016**, *8*, 2441−2448.
(27) Yim, C.; Sandwell, A.; Park, S. S. Hybrid Copper-Silver Conductive Tracks for Enhanced Oxidation Resistance under Flash Light Sintering. *ACS Appl. Mater. Interfaces* **2016**, *8*, 22369−22373.
(28) Huang, J.; Kaner, R. B. Flash Welding of Conducting Polymer Nanofibres. *Nat. Mater.* **2004**, *3*, 783−786.
(29) Yang, H. Y.; Hong, J.-M.; Kim, T. W.; Song, Y.-W.; Choi, W. K.; Lim, J. A. Split-Second Nanostructure Control of a Polymer:Fullerene Photoactive Layer Using Intensely Pulsed White Light for Highly Efficient Production of Polymer Solar Cells. *ACS Appl. Mater. Interfaces* **2014**, *6*, 1495−1501.
(30) Yang, H. Y.; Park, H.-W.; Kim, S. J.; Hong, J.-M.; Kim, T. W.; Kim, D. H.; Lim, J. A. Intense Pulsed Light Induced Crystallization of a Liquid-Crystalline Polymer Semiconductor for Efficient Production of Flexible Thin-Film Transistors. *Phys. Chem. Chem. Phys.* **2016**, *18*, 4627−4634.
(31) Lu, G.; Blakesley, J.; Himmelberger, S.; Pingel, P.; Frisch, J.; Lieberwirth, I.; Salzmann, I.; Oehzelt, M.; Di Pietro, R.; Salleo, A.; Koch, N.; Neher, D. Moderate Doping Leads to High Performance of Semiconductor/Insulator Polymer Blend Transistors. *Nat. Commun.* **2013**, *4*, 1588.
(32) Cosseddu, P.; Tiddia, G.; Milita, S.; Bonfiglio, A. Continuous Tuning of The Mechanical Sensitivity of Pentacene OTFTs on Flexible Substrates: From Strain Sensors to Deformable Transistors. *Org. Electron.* **2013**, *14*, 206−211.
(33) Kim, S. H.; Nam, S.; Jang, J.; Hong, K.; Yang, C.; Chung, D. S.; Park, C. E.; Choi, W.-S. Effect of the Hydrophobicity and Thickness of Polymer Gate Dielectrics on the Hysteresis Behavior of Pentacene-Based Field-Effect Transistors. *J. Appl. Phys.* **2009**, *105*, 104509.
(34) Gan, S. N.; Tan, B. Y. FTIR Studies of the Curing Reactions of Palm Oil Alkyd−Melamine Enamels. *J. Appl. Polym. Sci.* **2001**, *80*, 2309−2315.
(35) Ajayan, P. M.; Terrones, M.; de la Guardia, A.; Huc, V.; Grobert, N.; Wei, B. Q.; Lezec, H.; Ramanath, G.; Ebbesen, T. W. Nanotubes in a Flash–Ignition and Reconstruction. *Science* **2002**, *296*, 705−705.
(36) Srinivasan, C. Generation of Hydrogen by Splitting of Water Confined in Carbon Nanotubes with a Camera Flash. *Curr. Sci.* **2006**, *90*, 756−757.
(37) Wang, N.; Yao, B. D.; Chan, Y. F.; Zhang, X. Y. Enhanced Photothermal Effect in Si Nanowires. *Nano Lett.* **2003**, *3*, 475−477.

DOI: 10.1021/acsami.6b14957
ACS Appl. Mater. Interfaces 2017, 9, 11721−11731

(38) Xu, L.; Cheng, L.; Wang, C.; Peng, R.; Liu, Z. Conjugated Polymers for Photothermal Therapy of cancer. *Polym. Chem.* **2014**, *5*, 1573−1580.
(39) Yang, H.; Kim, S. H.; Yang, L.; Yang, S. Y.; Park, C. E. Pentacene Nanostructures on Surface-Hydrophobicity-Controlled Polymer/SiO_2 Bilayer Gate-Dielectrics. *Adv. Mater.* **2007**, *19*, 2868−2872.
(40) Kim, S. H.; Jang, M.; Yang, H.; Park, C. E. Effect of Pentacene-Dielectric Affinity on Pentacene Thin Film Growth Morphology in Organic Field-Effect Transistors. *J. Mater. Chem.* **2010**, *20*, 5612−5620.
(41) Hwang, M.; Lee, H. S.; Jang, Y.; Cho, J. H.; Lee, S.; Kim, D. H.; Cho, K. Effect of Curing Conditions of a Poly(4-vinylphenol) Gate Dielectric on the Performance of a Pentacene-Based Thin-Film Transistor. *Macromol. Res.* **2009**, *17*, 436−440.
(42) Yagi, I.; Tsukagoshi, K.; Aoyagi, Y. Modification of the Electric Conduction at the Pentacene/SiO2 Interface by Surface Termination of SiO2. *Appl. Phys. Lett.* **2005**, *86*, 103502.
(43) Fang-Chung, C.; Ying-Pin, C.; Yu-Jen, H.; Shang-Chieh, C. Morphological Study on Pentacene Thin-Film Transistors: the Influence of Grain Boundary on the Electrical Properties. *J. Phys. D: Appl. Phys.* **2010**, *43*, 405103.
(44) Kim, D. I.; Hwang, B. U.; Park, J. S.; Jeon, H. S.; Bae, B. S.; Lee, H. J.; Lee, N. E. Mechanical Bending of Flexible Complementary Inverters Based on Organic and Oxide Thin-Film Transistors. *Org. Electron.* **2012**, *13*, 2401−2405.
(45) Sokolov, A. N.; Cao, Y.; Johnson, O. B.; Bao, Z. Mechanistic Considerations of Bending-Strain Effects within Organic Semiconductors on Polymer Dielectrics. *Adv. Funct. Mater.* **2012**, *22*, 175−183.
(46) Yi, M.; Guo, Y.; Guo, J.; Yang, T.; Chai, Y.; Fan, Q.; Xie, L.; Huang, W. The Mechanical Bending Effect and Mechanism of High Performance and Low-Voltage Flexible Organic Thin-Film Transistors with a Cross-linked PVP Dielectric Layer. *J. Mater. Chem. C* **2014**, *2*, 2998−3004.
(47) Fang-Chung, C.; Tzung-Da, C.; Bing-Ruei, Z.; Ya-Wei, C. Influence of Mechanical Strain on the Electrical Properties of Flexible Organic Thin-Film Transistors. *Semicond. Sci. Technol.* **2011**, *26*, 034005.
(48) Deligöz, H.; Yalcinyuva, T.; Özgümüs, S.; Yildirim, S. Preparation, Characterization and Dielectric Properties of 4,4-Diphenylmethane Diisocyanate (MDI) Based Cross-linked Polyimide Films. *Eur. Polym. J.* **2006**, *42*, 1370−1377.
(49) Zhang, S.; Li, Y.; Ma, T.; Zhao, J.; Xu, X.; Yang, F.; Xiang, X.-Y. Organosolubility and Optical Transparency of Novel Polyimides Derived from 2[Prime or Minute],7[Prime or Minute]-bis(4-Aminophenoxy)-spiro(Fluorene-9,9[Prime or Minute]-Xanthene). *Polym. Chem.* **2010**, *1*, 485−493.

DOI: 10.1021/acsami.6b14957
ACS Appl. Mater. Interfaces 2017, 9, 11721−11731